Extracorporeal shock waves trigger tenogenic differentiation of human adipose-derived stem cells

[1]Letizia Rinella, [1]Francesca Marano, [1]Laura Paletto, [2]Marco Fraccalvieri, [1]Laura Annaratone, [1]Isabella Castellano, [3]Nicoletta Fortunati, [4]Alessandro Bargoni, [5]Laura Berta, [1]Roberto Frairia, [1]Maria Graziella Catalano.

[1]Department of Medical Sciences, University of Turin, Turin, Italy; [2]Plastic Surgery Unit, University of Turin, Turin, Italy; [3]Oncological Endocrinology, AO Città della Salute e della Scienza di Torino, Turin, Italy; [4]Department of Surgical Sciences, University of Turin, Turin, Italy; [5]Med & Sport 2000 Srl, Turin, Italy.

Corresponding Author: Maria Graziella Catalano, Department of Medical Sciences, University of Turin, Via Genova 3, 10126 Turin, Italy; tel. +39 011 670.5360; fax. +39 011 670.5366; mail: mariagraziella.catalano@unito.it

Running Head: Shockwaves and tendon differentiation

Abstract

Purposes: Incomplete tendon healing impairs the outcome of tendon ruptures and tendinopathies. Human Adipose-derived Stem Cells (hASCs) are promising for tissue engineering applications. Extracorporeal Shock Waves (ESW) are a leading choice for the treatment of several tendinopathies. In this study we investigated the effects of ESW treatment and tenogenic medium on the differentiation of hASCs into tenoblast-like cells. ***Materials and Methods:*** hASCs were treated with ESW generated by a piezoelectric device and tenogenic medium. Quantitative real-time PCR was used to check mRNA expression levels of tenogenic transcription factors, extracellular matrix proteins, and integrins. Western blot and immunofluorescence were used to detect collagen 1 and fibronectin. Collagen fibers were evaluated by Masson staining. Calcium deposition was assessed by Alizarin Red staining. ***Results:*** The combined treatment improved the expression of the tendon transcription factors scleraxis and eyes absent 2, and of the extracellular matrix proteins fibronectin, collagen I, and tenomodulin. Cells acquired elongated and spindle shaped fibroblastic morphology; Masson staining revealed the appearance of collagen fibers. Finally, the combined treatment induced the expression of alpha 2, alpha 6 and beta 1 integrin subunits, suggesting a possible role in mediating ESW effects. ***Conclusions:*** ESW in combination with tenogenic medium improved the differentiation of hASCs towards tenoblast-like cells, providing the basis for ESW and hASCs to be used in tendon tissue engineering.

Keywords: tendons; adipose-derived stem cells; extracorporeal shock waves; tenoblast differentiation; tissue engineering

Introduction

Tendon injuries and diseases are very common. Unfortunately, due to low cellularity and vascularization, tendon healing is often incomplete (1), and, to date, surgical treatments remain unsatisfactory (2). To overcome these limitations, cell therapy-based tissue engineering has now emerged as a potential alternative approach in the treatment of tendon diseases. Adult mesenchymal stem cells (MSCs) are multipotent lineages capable of differentiating into specialized tissues such as bone, cartilage, tendon, and ligaments; and for this reason, they have been proposed for tissue engineering to enhance tendon healing (3). MSCs can be extracted from bone marrow; but other sources have also been identified. Among these, adipose tissue represents an abundant source of MSCs with potential regenerative properties (4). Human Adipose-derived Stem Cells (hASCs) may therefore be considered as a powerful tool for treating tendinopathies (5), and very recently it has been demonstrated that a tenomodulin positive subpopulation of ASC is a promising source of tendon progenitor cells (6). Moreover, tenocytes respond to mechanical loading by modulating the extracellular environment through the formation and degradation of matrix proteins via a process termed mechanotransduction (7). Extracorporeal Shock Waves (ESW) are transient short-term acoustic pulses with high peak pressure and a very short rise time to peak pressure of the order of magnitude of nanoseconds and short pulse duration. ESW technology has been used in clinical practice since the 1980s, when it was first employed to break up kidney stones (8). More recently, shockwave therapy has emerged as a leading choice for the treatment of several orthopedic diseases (9) and different disorders such as proximal plantar fasciopathy, lateral elbow tendinopathy, calcific tendinopathy of the shoulder and patellar tendinopathy are tendon diseases where ESW treatment is being used successfully (10).

Based on these observations, the aim of the present study was to investigate the effects of ESW treatment on the differentiation of hASCs into tenoblast-like cells.

Materials and methods

Isolation, characterization and tenogenic differentiation of hASCs

hASCs were isolated from the waste subcutaneous-adipose tissue of 5 healthy female donors [range 30–50 years, body mass index (BMI) <30 without any pathological obesity], undergoing elective liposuction, after written consent and Institutional Review Board authorization. Primary cultures were established following the procedure of Zuc et al 2001 (4). Briefly, after digestion of raw lipoaspirates (50–100ml) with 0.075% type I collagenase (Sigma–Aldrich, Saint Louis, MO, USA) for 30 min, hASCs were separated by centrifugation (2100 x *g* for 10 min), filtered and plated in basal medium, consisting of Dulbecco's modified Eagle's Medium (DMEM/F12) (Lonza; Switzerland) plus 10% fetal bovine serum (FBS) and with the addition of 50 U/mL penicillin and 50 μg/mL streptomycin (all from GIBCO, Invitrogen Corp., Grand Island, NY, USA).

hASCs at passage 4 were investigated by flow cytometry analysis for the expression of surface antigens. In details, cells were detached by 0.5% trypsin/0.2% EDTA (Sigma–Aldrich, Saint Louis, MO, USA); thereafter, the cells were washed with cold PBS (Phosphate Buffer Saline) (Sigma–Aldrich, Saint Louis, MO, USA) and then resuspended in cold PBS plus 0.1% BSA (Bovine Serum Albumin) (Sigma–Aldrich, Saint Louis, MO, USA). The cells were incubated for 30 minutes in ice, using the following phycoerythrin (PE) or fluorescein isothiocyanate (FITC)-conjugated antibodies: mouse anti-human CD13, CD14 and CD34 (BD Biosciences, Franklin Lakes, NJ, USA); mouse anti-human CD45, CD90, CD105 and CD44 (Immunotech, Marseille, France). At the end of the incubation, two washings with cold PBS plus 0.1% of BSA were performed. Ten thousand events were acquired for each surface marker on flow cytometer (EPICS XL, Coulter Corp., Hialeah, FL, USA).

To induce tendon cell differentiation, hASCs were cultured in tenogenic medium consisting of basal medium supplemented with 50ng/ml human Insulin-like Growth Factor-I (IGF-1) and 10ng/ml human Transforming Growth Factor beta 1 (TGF-β1) (11). hASCs cultured in basal medium were used as controls.

P*rimary cultures of human tenocytes: isolation and expansion*

Discarded fragments of semitendinosus tendons were collected from 2 healthy young donors (mean age = 23 ± 7 y) who underwent arthroscopic anterior cruciate ligament reconstruction with autologous hamstrings at our hospital. All patients gave written consent to the procedure and all procedures were carried out with institutional review board approval. Tenocytes were isolated following the procedure by Kraus et al. (12) with minor modifications. Tendon tissues were minced and enzymatically digested with 0.25% trypsin in DMEM/F12 overnight at 4°C. Subsequently, thy were treated with 0.3% type I collagenase in DMEM/F12 with continuous agitation for 1h at 37°C. The isolated nucleated cells were then cultured in basal medium consisting of DMEM/F12 plus 10% FBS, with 50 U/mL penicillin and 50 μg/mL streptomycin. Cell cultures were maintained at 37°C in a humidified atmosphere with 5% CO_2; the culture medium was changed every 3 days. When cells reached 80–90% confluence, they were detached by incubation with 0.5% trypsin/0.2% EDTA (Sigma–Aldrich, Saint Louis, MO, USA) and then expanded at a density of 5×10^3 cells/cm^2. RNA and proteins were extracted from tenocytes at passages 2 to 4, to be used as positive controls in gene expression, western blots and immunofluorescence experiments.

ESW treatment

The shockwave generator utilized for hASC treatments is a piezoelectric device (Piezoson 100; Richard Wolf, Knittlingen, Germany), especially designed for clinical use in orthopaedics and traumatology. The experimental set-up has been reported previously (13). Briefly, 1 ml aliquots of hASC cell suspension adjusted to 1×10^6 cell/ml were placed in 20mm polypropylene tubes (Nunc, Wiesbaden, Germany), which were then completely filled with culture medium. Subsequently, cells were gently pelleted by centrifugation at 250 x *g* in order to minimize motion during shockwave treatment. Each cell-containing tube was placed in vertical alignment with the focal area and was adjusted so that the central point of the focal area corresponded to the centre of the tube bottom. The shockwave unit was kept in contact with the cell containing tube by means of a water-filled cushion. Common ultrasound gel was used as a contact medium between cushion and tube. hASC

cells were treated as follows: 1) control cells maintained in DMEM/F12 plus FBS 10% (Basal); 2) ESW-treated cells (Energy Flux Density, EFD=0.32mJ/mm^2; peak positive pressure 90 MPa) receiving a number of 1000 shots (frequency = 4 shocks/s) and maintained in DMEM/F12 plus FBS 10% (ESW); 3) cells maintained in tenogenic medium (TENO); 4) ESW-treated cells (EFD=0.32mJ/mm^2; 1000 shots) maintained in tenogenic medium (TENO ESW).

Cell viability

After treatments as above, cells were seeded at 3×10^3 cells/well in 96-well plates (Corning, New York, NY, USA). At 1, 3, 5, 7 and 9 days, cell viability was assessed using the Cell Proliferation Reagent WST-1 (Roche Applied Science, Penzberg, Germany), following the manufacturer's instructions. This is a colorimetric assay for the quantification of cell viability and proliferation, based on the cleavage of the tetrazolium salt WST-1 by mitochondrial dehydrogenases of viable cells. Briefly, 10 µl of WST-1 were added to each well. After 1-h incubation, absorbance at 450 nm was measured using a plate reader (Model 680 Microplate Reader; Bio-Rad, Laboratories S.r.l., Milan, Italy). Four replicate wells were used to determine each data point.

Cell Morphology

After 72 hours of treatment, cell morphology was observed under Diavert inverted light microscope (Leitz, Wetzlar, Germany); photos were taken at x200 magnifications by Leica DC100 digital camera system (Microsystems,Wetzlar, Germany) using Leica Qwin as software for image processing.

Gene expression

At defined times after treatment, total RNA was extracted from hASCs and primary tenocytes using TRIzol Reagent (Invitrogen Ltd, Paisley, UK). DNase I was added to remove remaining genomic DNA. 1 µg sample of total RNA was reverse-transcribed with iScript cDNA Synthesis Kit (Bio-Rad Laboratories S.r.l., Milan, Italy) following manufacturer's protocol. Primers (Table S1) were designed using Beacon Designer 5.0 software according to parameters outlined in the Bio-Rad iCycler Manual. The specificity of primers was confirmed by BLAST analysis. Real-time

polymerase chain reaction was performed using a BioRad iQ iCycler Detection System (Bio-Rad Laboratories S.r.l., Milan, Italy) with SYBR green fluorophore. Reactions were performed in a total volume of 25 μl containing 12.5 μl IQ SYBR Green Supermix (Bio-Rad Laboratories S.r.l., Milan, Italy), 1 μl of each primer at 10 μM concentration, and 5 μl of the previously reverse-transcribed cDNA template. The protocol used is as follows: denaturation (95°C for 5 min), amplification repeated 40 times (95°C for 15 s, 60°C for 30 s). A melting curve analysis was performed following every run to ensure a single amplified product for every reaction. All reactions were carried out at least in triplicate for each sample. Results were normalized using the geometric mean for three different housekeeping genes (β-actin and ribosomal protein L13A and RPLPO) and expressed as relative expression fold vs untreated controls (Basal).

Immunofluorescence microscopy

After different treatments, cells (2×10^3) were seeded in 96-well plates (Corning, New York, NY, USA). After 1 and 4 weeks, cells were fixed in acetone/methanol (1:1) at 4°C for 20 minutes, permeabilized with PBS containing 0.5% Triton X-100, 0.05% NaN_3 and incubated with the following antibodies: polyclonal sheep anti-type I collagen (COL1, 2 μg/ml, R&D Systems, Minneapolis, MN, USA) and polyclonal rabbit anti-fibronectin 1 (FN1, 1:500, Sigma–Aldrich, Saint Louis, MO, USA), at 4°C overnight. Detection with secondary antibodies was as follows: for COL1, anti-sheep conjugated with Alexa Fluor 594 (1:500, Invitrogen, San Diego, CA, USA) and for FN1, anti-rabbit conjugated with cy3 (1:1000, GE Healthcare Europe, Milan, Italy). Nuclear staining was obtained by Hoechst 33258 [500 ng/ml in dimethylsulphoxide (DMSO)] in PBS. Cells were washed twice with distilled water. Cells were observed by inverted microscope Leica DMI 4000 B (Leica Microsystems, Wetzlar, Germany) and photos of single channels and overlayers at x200 magnifications, were taken by Leica DCF340 FX digital camera system (Leica Microsystems, Wetzlar, Germany). Fluorescence was quantified using ImageJ (version 1.48, NIH, Bethesda, Maryland) imaging software.

Immunoblotting

At different times after treatments, cell culture media were recovered and both hASC cells and tenocytes were scraped from the flask in the presence of 1 mL lysis buffer (50 mM Tris–HCl pH 7.5, 150 mM NaCl, 1 mM EDTA, 1 mM EGTA, 0.5% sodium deoxycholate, 1% Nonidet P-40, 0.1% SDS, 10 mg/mL PMSF, 30 L/mL aprotinin, and 100 mM sodium orthovanadate). Cell lysates were incubated in ice for 30–60 minutes. At completion, tubes were centrifuged at 4 °C for 20 minutes at 15,000 x g. Media and cell lysates were separated on SDS-PAGE, transferred to PVDF and probed with the following antibodies: polyclonal anti-COL1 (1:800, R&D Systems, Minneapolis, MN), for culture media; polyclonal anti-FN1 (1:10000, Sigma–Aldrich, Saint Louis, MO, USA), for cell lysates. The membrane for FN1 was then stripped and reprobed with a mouse monoclonal anti-Tubulin antibody (1:10,000, Sigma–Aldrich, Saint Louis, MO, USA) to check protein loading. Red ponceau was used to confirm equal loading for type I collagen membrane. Proteins were detected with Pierce Super Signal chemiluminescent substrate. Bands were photographed and analyzed using Kodak 1D Image Analysis software.

Masson Trichrome staining

After different treatments, cells ($25x10^4$) were seeded on sterilized coverslips (22 x 22 mm) placed in 6 cm Petri dishes and kept in a humidified incubator with 5% CO_2 at 37°C.

After 4 weeks, the cells grown on coverslips were fixed in 4% neutral-buffered formalin for 10 min and dehydrated through a series of alcohols up to absolute alcohol. The slides were first stained in modified Harris's haematoxylin for 5 min; then, rinsed in lithium carbonate solution until the sections changed colour to blue. Subsequently, the slides were washed and stained in scarlet-acid fuchsine solution for 7-10 min. The slides were rinsed in a 1% acetic acid solution and immersed in phosphomolybdic acid for 4-5 min. The sections were transferred to Light Green and stained for 7-10 min. After that, they were placed in 1% acetic acid solution. The slides were then dehydrated through 95% ethyl alcohol, absolute ethyl alcohol and cleared in xylene before being mounted. Slides were observed by microscope Leica DM2000 (Leica Microsystems, Wetzlar, Germany) and

photos were taken by Leica ICC50 HD digital camera system (Leica Microsystems, Wetzlar, Germany) at x200 final magnification. ImageJ (version 1.48, NIH, Bethesda, Maryland) imaging software was used to analyze Masson trichrome digital images and quantify the amount of collagen.

Alizarin Red staining

Calcium deposition was evaluated at 4 weeks by staining with 40 mM Alizarin Red-S (ARS, pH 4.1). After fixation in ethanol and washing with Tris-buffered saline, cells were stained with ARS for 15 min, washed with Tris-buffered saline and observed under light microscopy. Cells were observed under inverted microscope Leica DMI 3000 B (Leica Microsystems, Wetzlar, Germany) and photographed by Leica DCF310 FX digital camera system (Leica Microsystems, Wetzlar, Germany) at x400 final magnification.

Statistical analysis

Data are expressed throughout the text as means ± SD. The means were calculated from n=5 for hASCs, and n=2 for primary tenocytes, respectively. 3 technical replicates were used for each donor. Comparison between groups was performed with analysis of variance (two-way ANOVA) and the threshold of significance was calculated with the Bonferroni test. Statistical significance was set at $p<0.05$.

Results

hASC characterization

More than 95% of hASCs expressed CD13, CD44 and CD105, whereas a very low expression of CD14 (1%) and no expression of CD34 and CD45 was detected (Table S2). Moreover, a positivity of at least 95% for the same markers was also maintained in subsequent steps (data not shown). As we reported elsewhere (14,15), hASCs were able to differentiate into osteogenic and adipogenic lineages under specific culture conditions, confirming their differentiating potential.

ESW effect on cell viability and morphology

The energy level and number of shots used for ESW treatment (EFD =0.32 mJ/mm^2; peak positive pressure 90 MPa, 1000 shots) allowed a viability > 80% soon after treatment (Table S2) and did not modify cell growth up to 9 days (Figure 1, panel A).

Light microscopy was used to evaluate the differences in cell morphology in response to treatments (Figure 1, panel B). After 72 hours, cells in basal conditions exhibited a polygonal phenotype; on the contrary, combined treatment with tenogenic medium and ESW determined the appearance of an elongated and spindle shaped fibroblastic morphology.

Effects on tenogenic gene expression

As shown in Figure 2 (panels A and B), after 48 hours' treatment, tenogenic medium alone significantly increased the expression of the two transcription factor *scleraxis* (*SCX*) (panel A, TENO vs Basal: 3.5 times, $p<0.001$) and *eyes absent* 2 (*EYA2*) (panel B, TENO vs Basal: 2.5 times, $p<0.001$); but, the greatest effect was obtained by using the combined treatment with tenogenic medium and ESW (for *SCX*, panel A: TENO ESW vs Basal: 5.8 times, $p<0.001$; TENO ESW vs TENO: 1.8 times, $p<0.001$; for *EYA2*, panel B: TENO ESW vs Basal: 3.0 times, $p<0.001$; TENO ESW vs TENO: 1.2 times, $p<0.001$).

As both SCX and EYA2 regulate the expression of the tendon extracellular matrix proteins (16,17), we evaluated the expression of *fibronectin* (*FN1*), *type I collagen* (*COL1*) and *tenomodulin* (*TNMD*) at 7 days after treatment. Tenogenic medium significantly increased the expression of *FN1* (Figure

2, panel C, TENO vs Basal: 2.7 times, $p<0.001$), *COL1* (Figure 2, panel D, TENO vs Basal: 1.22 times, $p<0.05$), and *TNMD* (Figure 2, panel E, TENO vs Basal: 2.9 times, $p<0.01$); again the combined treatment determined the best effect (for *FN1*, panel C: TENO ESW vs Basal: 4.25 times, $p<0.001$; TENO ESW vs TENO: 1.6 times, $p<0.001$; for *COL1*, panel D: TENO ESW vs Basal: 1.36 times, $p<0.01$; TENO ESW vs TENO: 1.1 times, $p<0.05$; for *TNMD*, panel E: TENO ESW vs TENO: 4.5 times, $p<0.001$). Moreover, as far as tenomodulin expression is concerned, ESW treatment alone significantly increased its expression (panel E: ESW vs Basal: 2.5 times, $p<0.05$). Notably, after the combined treatment, levels of expression of both transcription factors as well as of the extracellular matrix proteins were comparable and even greater than those observed in primary culture of tenocytes, used as positive controls.

Effects on extracellular matrix protein deposition

The effect on the extracellular matrix proteins FN1 and COL1 was further confirmed by the evaluation of protein deposition.

Effects on FN1

After 7-day-treatments, tenogenic medium significantly increased FN1 production, as demonstrated by both immunofluorescence (Figure 3, panel A, TENO vs Basal, $p<0.01$) and western blotting (Figure 3, panels B and C, TENO vs Basal, $p<0.05$); but was the combination of tenogenic medium and ESW that gave the best result in terms of FN1 induction (immunofluorescence, Figure 3, panel A, TENO ESW vs Basal, $p<0.001$; TENO ESW vs TENO, $p<0.05$; western blotting, Figure 3, panels B and C, TENO ESW vs Basal, $p<0.001$; TENO ESW vs TENO, $p<0.01$).

Effects on COL1

The same behavior was also observed for COL1 production. In fact, after 7 days, already tenogenic medium alone significantly increased COL1 (immunofluorescence, Figure 4, panel A, TENO vs Basal, $p<0.001$; western blotting, Figure 4, panels B and C, TENO vs Basal, $p<0.001$); again, was the combination of tenogenic medium and ESW that gave the best results in terms of COL1 production (immunofluorescence, Figure 4, panel A, TENO ESW vs Basal, $p<0.001$; TENO ESW

vs TENO, $p<0.05$; western blotting, Figure 4, panels B and C, TENO ESW vs Basal, $p<0.001$; TENO ESW vs TENO, $p<0.01$).

In addition, the increased COL1 production was maintained up to five weeks, as demonstrated by immunofluorescence (Figure 5, panels A and B: TENO vs Basal $p<0.01$; TENO ESW vs Basal $p<0.001$; TENO ESW vs TENO $p<0.001$). Interestingly, at this time point the combined treatment (Figure 5, panel A) determined the formation of parallel collagen fibers, which play an important role in regulating tenoblast function and differentiation (18). Finally, the appearance of collagen fibers (arrows) was confirmed by Masson trichrome staining, as shown in Figure 5, panels C and D (TENO vs Basal $p<0.01$; TENO ESW vs Basal $p<0.001$; TENO ESW vs TENO $p<0.001$).

Effects on integrin expression

To get insights into the mechanisms involved in the effect of ESW in tenogenic differentiation, the expression of integrins involved in mechanotransduction was assessed. We evaluated the expression of *integrins α1, 2, 5, 6, 10, 11* and *V* and of *integrins β 1, 3, 5,* and *8*; the most expressed in tendons and ligaments (19). Among these, after 72 hours, the expression of *α2* (*ITGα2*), *α6* (*ITGα6*) and *β1* (*ITGβ1*) integrins, was affected by our experimental treatments, as shown in Figure 6. The expression of *ITGα2* (Figure 6, panel A) was significantly increased by ESW alone (ESW vs Basal: 4.7 times, $p<0.001$), by tenogenic medium (TENO vs Basal: 2.1 times, $p<0.05$) and by the combined treatment (TENO ESW vs Basal: 8 times, $p<0.001$) respectively. The latter was the most effective (TENO ESW vs ESW: 1.7 times, $p<0.001$; TENO ESW vs TENO: 3.8 times, $p<0.001$). The expression of *ITGα6* (Figure 6, panel B) was significantly increased by ESW alone (ESW vs Basal: 4.7 times, $p<0.001$), by tenogenic medium (TENO vs Basal: 1.9 times, $p<0.01$) and by the combined treatment (TENO ESW vs Basal: 5.9 times, $p<0.001$) respectively. The latter was the most effective (TENO ESW vs ESW: 1.3 times, $p<0.01$; TENO ESW vs TENO: 3.1 times, $p<0.01$). The expression of *ITGβ1* (Figure 6, panel C) was significantly increased by ESW alone (ESW vs Basal: 1.7 times, $p<0.01$) and by the combined treatment (TENO ESW vs Basal: 2.3 times,

296 $p<0.001$). The latter was again the most effective (TENO ESW vs ESW: 1.4 times, $p<0.05$; TENO
297 ESW vs TENO: 2.1 times, $p<0.001$).

298 ***Effects on osteogenic differentiation***

299 As we reported (14) that ESW treatment, especially when combined with specific osteogenic
300 medium, elicited the differentiation of hASCs towards osteoblast-like cells, we assessed whether the
301 combined treatment could lead to the osteogenic differentiation of hASCs. As reported in Figure 7,
302 the combined treatment with tenogenic medium and ESW had no effect on *bone morphogenetic*
303 *protein-2, BMP-2* (panel A), *runt-related transcription factor 2, Runx2* (panel B) and *alkaline*
304 *phosphatase, ALP* (panel C) expression and determined no production of calcium deposits (panel
305 D). Moreover, present data confirm our previous results (14) about the positive effect of ESW
306 treatment alone on the expression of *BMP-2, Runx2* and *ALP* and on calcium deposits.

307

Discussion

The present study demonstrates that ESW potentiate the effects of tenogenic medium on the differentiation of hASCs towards tenoblast-like cells, as evidenced by the up-regulation of specific gene markers, spindle-shaped cell morphology and extracellular matrix fiber deposition. These findings support the potency of combining stem cells, mechanical forces and biochemical factors to induce and sustain tendon differentiation and regeneration.

Since their first description by Zuk et al. (4), it is well known that ASCs are at least as efficient as bone marrow-derived stem cells when used in tissue engineering; moreover, the low donor site morbidity and high rate of growth during culturing, make them an ideal cell type to be used in regenerative medicine. ASCs have been successfully used in *in vivo* models of tendon repair (20) and some Authors reported that ASCs work better than bone marrow stem cells in *in vivo* tendon injury models (21). Moreover, it has been described that ASC source can be biochemically induced towards tenogenic commitment, validating its potential for tendon regeneration strategies (22). Accordingly, in our *in vitro* model, tenogenic medium increased the expression of specific tendon genes and determined collagen and fibronectin deposition.

Here we demonstrate that mechanical stimulation with ESW enhances the biochemical effects of a containing-growth factor specific medium to drive hASCs towards a tenoblast-like phenotype. Our results are in line with previous reports about the role of mechanical forces in tendon healing and stem cell differentiation towards tenoblasts. Pulsed electromagnetic fields influence the proliferation, tendon-specific marker expression and release of anti-inflammatory cytokines and angiogenic factors of healthy human tendon cells (23). Cyclic tension promotes fibroblastic differentiation of stem cells seeded on fibrous collagen-based scaffolds (24) and stem cell differentiation toward tenocytes (25, 26). Moreover, the combination of the tendon transcription factor scleraxis and mechanical stress synergistically drives differentiation of human embryonic stem cells to induce teno-lineage commitment (27).

As far as the biological effects of ESW therapy on tendon healing are concerned, several experimental studies on animal models have been performed (28-34), suggesting a role of ESW in determining the activation of a complex network of molecules acting on collagen synthesis and angiogenesis. On the contrary, to date only two studies from the same group described the effects of ESW *in vitro* on human healthy and ruptured tendon-derived tenocytes (35, 36) and another study demonstrated that soft-focused ESW treatment was able to induce positive modulation of cell viability, proliferation and tendon-specific marker expression, as well as release of anti-inflammatory cytokines (37). However, to date no other study investigated the possibility of ESW to facilitate the differentiation of human mesenchymal stem cells towards tenocytes.

As far as gene expression is concerned, a panel of genes typically expressed by tendons was increased by the combined treatment. We observed an enhanced expression of the transcription factor scleraxis, which is the only direct molecular regulator of tenocyte differentiation identified and expressed in tendon progenitors (38). Moreover, the combined treatment with tenogenic medium and ESW induced the expression of the tendon extracellular matrix proteins fibronectin and type I collagen. Type I collagen is the most abundant protein in healthy tendon tissue (39). Notably, the combined treatment antagonized the ESW-induced BMP-2 expression, which is known to stimulate osteogenesis in both hASCs (18) and in tendon-derived stem cells (40). As a consequence, no increase of Runx2 and ALP and no production of calcium deposits were observed. Nevertheless, being the present an *in vitro* study, only future work in animal models will definitively exclude any potential effect of the combined treatment on ectopic calcification of tendons.

Integrins mediate cell–matrix interactions and are the transducers of the mechanochemical information between extracellular and intracellular compartments (41). Present work suggests an involvement of integrins as possible mediators of ESW effects at cellular and molecular levels. In fact, ESW increased the expression of $\alpha 2$, $\beta 1$ and $\alpha 6$ subunits. $\alpha 2/\beta 1$ integrin is a receptor for laminin, collagen, and fibronectin (19). It is responsible for cell adhesion to collagens, modulation

of collagen and collagenase gene expression, force generation and organization of newly synthesized extracellular matrix (42). The α6 subunit, expressed in vascular structures in the healing ligaments (43) and in the healing tendons (44), is involved in vasculogenesis.

In conclusion, the novelty of the present work is the ability of ESW to boost the process of hASC differentiation towards tenoblast-like cells induced by tenogenic medium, supporting a role for ESW as a new tool to be used in combination with ASC in tendon tissue engineering.

Funding

The study was supported by Fondazione CRT Turin, Italy and by "Fondi per la Ricerca Locale", University of Turin, Italy.

Declaration of interests

The authors report no conflicts of interest. The authors alone are responsible for the content and writing of the article.

Acknowledgments

We thank Med & Sport 2000 S.r.l., Turin, Italy for providing the shock wave generator; Cristina Grange for staining experiments, Gillian Lynch for English editing.

References

1. Liu CF, Aschbacher-Smith L, Barthelery NJ, Dyment N, Butler D, Wylie C. What we should know before using tissue engineering techniques to repair injured tendons: a developmental biology perspective. Tissue Eng Part B Rev 2011;17:165-176.
2. Voleti PB, Buckley MR, Soslowsky LJ. Tendon healing: repair and regeneration. Annu Rev Biomed Eng 2012;14:47-71.
3. Grange S. Current issues and regulations in tendon regeneration and musculoskeletal repair with mesenchymal stem cells. Curr Stem Cell Res Ther 2012;7:110-114.
4. Zuk PA, Zhu M, Mizuno H, Huang J, Futrell JW, Katz AJ, Benhaim P, Lorenz HP, Hedrick MH. Multilineage cells from human adipose tissue: implications for cell-based therapies. Tissue Eng 2001;7:211-228.
5. Uysal AC, Mizuno H. Tendon regeneration and repair with adipose derived stem cells. Curr Stem Cell Res Ther 2010;5:161-167.
6. Gonçalves AI, Gershovich PM, Rodrigues MT, Reis RL, Gomes ME. Human adipose tissue-derived tenomodulin positive subpopulation of stem cells: A promising source of tendon progenitor cells. J Tissue Eng Regen Med. 2017 Jun 7. doi: 10.1002/term.2495.
7. Wang JH. Mechanobiology of tendon. J Biomech 2006;39:1563-1582.
8. Sturtevant B. 'Shock waves physic of lithotriptors' in Smith's Textbook of endourology. Smith A, Badlani GH, Bagley DH, eds, St Louis, MO, Quality Medical Publishing 1996.
9. Wang CJ. Extracorporeal shockwave therapy in musculoskeletal disorders. J Orthop Surg Res 2012;7:11.
10. Ioppolo F, Rompe JD, Furia JP, Cacchio A. Clinical application of shock wave therapy (SWT) in musculoskeletal disorders. Eur J Phys Rehabil Med 2014;50:217-230.
11. Theiss F, Mirsaidi A, Mhanna R, Kümmerle J, Glanz S, Bahrenberg G, Tiaden AN, Richards PJ. Use of biomimetic microtissue spheroids and specific growth factor

supplementation to improve tenocyte differentiation and adaptation to a collagen-based scaffold in vitro. Biomaterials 2015;69:99-109.

12. Kraus A, Woon C, Raghavan S, Megerle K, Pham H, Chang J. Co-culture of human adipose-derived stem cells with tenocytes increases proliferation and induces differentiation into a tenogenic lineage. Plast Reconstr Surg 2013;132:754e-766e.
13. Frairia R, Catalano MG, Fortunati N, Fazzari A, Raineri M, Berta L. High energy shock waves (HESW) enhance paclitaxel cytotoxicity in MCF-7 cells. Breast Cancer Res Treat 2003;81:11-19.
14. Rinella L, Marano F, Berta L, Bosco O, Fraccalvieri M, Fortunati N, Frairia R, Catalano MG. Extracorporeal shock waves modulate myofibroblast differentiation of adipose-derived stem cells. Wound Repair Regen 2016;24:275-286.
15. Catalano MG, Marano F, Rinella L, de Girolamo L, Bosco O, Fortunati N, Berta L, Frairia R. Extracorporeal shockwaves (ESW) enhance the osteogenic medium-induced differentiation of adipose-derived stem cells into osteoblast-like cells. J Tissue Eng Regen Med 2017;11:390-399.
16. Alberton P, Popov C, Prägert M, Kohler J, Shukunami C, Schieker M, Docheva D. Conversion of human bone marrow-derived mesenchymal stem cells into tendon progenitor cells by ectopic expression of scleraxis. Stem Cells Dev 2012;21:846-858.
17. Xu PX, Cheng J, Epstein JA, Maas RL. Mouse Eya genes are expressed during limb tendon development and encode a transcriptional activation function. Proc Natl Acad Sci U S A 1997;94:11974-11979.
18. Nguyen TD, Liang R, Woo SL, Burton SD, Wu C, Almarza A, Sacks MS, Abramowitch S. Effects of cell seeding and cyclic stretch on the fiber remodeling in an extracellular matrix-derived bioscaffold. Tissue Eng Part A 2009;15:957-963.
19. Docheva D, Popov C, Alberton P, Aszodi A. Integrin signaling in skeletal development and function. Birth Defects Res C Embryo Today 2014;102:13-36.

20. Behfar M, Sarrafzadeh-Rezaei F, Hobbenaghi R, Delirezh N, Dalir-Naghadeh B. Adipose derived stromal vascular fraction improves early tendon healing: an experimental study in rabbits. Vet Res Forum 2011;2:248–253.
21. Behfar M, Javanmardi S, Sarrafzadeh-Rezaei F. Comparative study on functional effects of allotransplantation of bone marrow stromal cells and adipose derived stromal vascular fraction on tendon repair: a biomechanical study in rabbits. Cell J 2014;16:263-270.
22. Gonçalves AI, Rodrigues MT, Lee SJ, Atala A, Yoo JJ, Reis RL, Gomes ME. Understanding the role of growth factors in modulating stem cell tenogenesis. PLoS One 2013;8:e83734.
23. de Girolamo L, Stanco D, Galliera E, Viganò M, Colombini A, Setti S, Vianello E, Corsi Romanelli MM, Sansone V. Low frequency pulsed electromagnetic field affects proliferation, tissue-specific gene expression, and cytokines release of human tendon cells. Cell Biochem Biophys 2013;66:697-708.
24. Qiu Y, Lei J, Koob TJ, Temenoff JS. Cyclic tension promotes fibroblastic differentiation of human MSCs cultured on collagen-fibre scaffolds. J Tissue Eng Regen Med 2016;10:989-999.
25. Morita Y, Watanabe S, Ju Y, Xu B. Determination of optimal cyclic uniaxial stretches for stem cell-to-tenocyte differentiation under a wide range of mechanical stretch conditions by evaluating gene expression and protein synthesis levels. Acta Bioeng Biomech 2013;15:71-79.
26. Nam HY, Pingguan-Murphy B, Amir Abbas A, Mahmood Merican A, Kamarul T. The proliferation and tenogenic differentiation potential of bone marrow-derived mesenchymal stromal cell are influenced by specific uniaxial cyclic tensile loading conditions. Biomech Model Mechanobiol 2015;14:649-663.

27. Chen X, Yin Z, Chen JL, Shen WL, Liu HH, Tang QM, Fang Z, Lu LR, Ji J, Ouyang HW. Force and scleraxis synergistically promote the commitment of human ES cells derived MSCs to tenocytes. Sci Rep 2012;2:977.
28. Rompe JD, Kirkpatrick CJ, Kullmer K, Schwitalle M, Krischek O. Dose-related effects of shock waves on rabbit tendo Achillis. A sonographic and histological study. J Bone Joint Surg Br 1998;80:546-552.
29. Maier M, Tischer T, Milz S, Weiler C, Nerlich A, Pellengahr C, Schmitz C, Refior HJ. Dose-related effects of extracorporeal shock waves on rabbit quadriceps tendon integrity. Arch Orthop Trauma Surg 2002;122:436-441.
30. Orhan Z, Cam K, Alper M, Ozturan K. The effects of extracorporeal shock waves on the rat Achilles tendon: is there a critical dose for tissue injury? Arch Orthop Trauma Surg 2004; 124:631-635.
31. Kersh KD, McClure SR, Van Sickle D, Evans RB. The evaluation of extracorporeal shock wave therapy on collagenase induced superficial digital flexor tendonitis. Vet Comp Orthop Traumatol 2006;19:99-105.
32. Bosch G, de Mos M, van Binsbergen R, van Schie HT, van de Lest CH, van Weeren PR. The effect of focused extracorporeal shock wave therapy on collagen matrix and gene expression in normal tendons and ligaments. Equine Vet J 2009;41:335-341.
33. Zhang D, Kearney CJ, Cheriyan T, Schmid TM, Spector M. Extracorporeal shockwave-induced expression of lubricin in tendons and septa. Cell Tissue Res 2011;346:255-262.
34. Yoo SD, Choi S, Lee, GJ, Chon J, Jeong YS, Park HK, Kim HS. Effects of extracorporeal shockwave therapy on nanostructural and biomechanical responses in the collagenase induced Achilles tendinitis animal model. Lasers Med Sci 2012;27:1195-1204.
35. Vetrano M, d'Alessandro F, Torrisi MR, Ferretti A, Vulpiani MC, Visco V. Extracorporeal shock wave therapy promotes cell proliferation and collagen synthesis of primary cultured human tenocytes. Knee Surg Sports Traumatol Arthrosc 2011;19:2159-2168.

36. Leone L, Vetrano M, Ranieri D, Raffa S, Vulpiani MC, Ferretti A, Torrisi MR, Visco V. Extracorporeal Shock Wave Treatment (ESWT) improves in vitro functional activities of ruptured human tendon-derived tenocytes. PLoS One 2012;7:e49759.
37. de Girolamo L, Stanco D, Galliera E, Viganò M, Lovati AB, Marazzi MG, Romeo P, Sansone V. Soft-focused extracorporeal shock waves increase the expression of tendon-specific markers and the release of anti-inflammatory cytokines in an adherent culture model of primary human tendon cells. Ultrasound Med Biol 2014;40:1204-1215.
38. Omachi T, Sakai T, Hiraiwa H, Hamada T, Ono Y, Nakashima M, Ishizuka S, Matsukawa T, Oda T, Takamatsu A, Yamashita S, Ishiguro N. Expression of tenocyte lineage-related factors in regenerated tissue at sites of tendon defect. J Orthop Sci 2015;20:380-389.
39. Heckman DS, Gluck GS, Parekh SG. Tendon disorders of the foot and ankle, part 2: Achilles tendon disorders. Am J Sports Med 2009;37:1223–1234.
40. Rui YF, Lui PP, Ni M, Chan LS, Lee YW, Chan KM. Mechanical loading increased BMP-2 expression which promoted osteogenic differentiation of tendon-derived stem cells. J Orthop Res 2011;29:390-396.
41. Berrier AL, Yamada KM. Cell–matrix adhesion. J Cell Physiol 2007;213:565–573.
42. Schiro JA, Chan BMC, Roswit WT, Kassner PD, Pentland AP, Hemler ME, Eisen AZ, Kupper TS. Integrin $\alpha 2\beta 1$ (VLA-2) mediates reorganization and contraction of collagen matrices by human cells. Cell 1991;67:403-410.
43. Schreck PJ, Kitabayashi LR, Amiel D, Akeson WH, Woods VL Jr. Integrin display increases in the wounded rabbit medial collateral ligament but not the wounded anterior cruciate ligament. J Orthop Res 1995;13:174-183.
44. Harwood FL, Monosov AZ, Goomer RS, Gelberman RH, Winters SC, Silva MJ, Amiel D. Integrin expression is upregulated during early healing in a canine intrasynovial flexor tendon repair and controlled passive motion model. Connect Tissue Res1998;39:309-316

505 **Figure Legends**

506 **Figure 1. Effects on cell viability (panel A).** Basal, ESW, TENO and TENO ESW-treated h ASC
507 cells were cultured up to 9 days. At 1, 3, 5, 7 and 9 days, cell viability was determined by the
508 WST-1 method, and expressed as ratio vs day 0. **Effects on cell morphology (panel B).**
509 Morphology of Basal, ESW, TENO and TENO ESW-treated hASC cells. Magnification x200.

510 **Figure 2. Effects on tendon-specific gene expression.** mRNA expression of SCX (panel A),
511 EYA2 (panel B), FN1 (panel C), COL1 (panel D) and TNMD (panel E) was evaluated by RT-PCR.
512 Results are normalized for three different housekeeping genes (β-actin, RPLPO and L13A) and
513 expressed as relative expression fold *vs* Basal. Significance vs Basal: *, $p<0.05$; ***, $p<0.001$.
514 Significance TENO ESW vs TENO: °, $p<0.05$; °°°, $p<0.001$.

515 **Figure 3. Effects on fibronectin.** Immunofluorescence for FN1 (panel A**)** in Basal, ESW, TENO
516 and TENO ESW-treated hASC cells after 7 days. Magnification x200. FN1 fluorescence
517 quantification. Significance vs Basal: ***, $p<0.001$. Significance TENO ESW vs TENO: °, $p<0.05$.
518 Immunoblotting for fibronectin (panel B) in Basal, ESW, TENO and TENO ESW-treated hASC
519 cells. Anti-Tubulin antibody was used to confirm equal loading. Blot is representative of five
520 independent experiments. Semiquantitative analysis of immunoblotting results (panel C).
521 Significance vs Basal: *, $p<0.05$; ***, $p<0.001$. Significance TENO ESW vs TENO: °°, $p<0.01$.
522 Tenocytes were used as positive controls.

523 **Figure 4. Effects on type I collagen after 7 days.** Immunofluorescence for COL1 (panel A**)** in
524 Basal, ESW, TENO and TENO ESW-treated h ASC cells. Magnification x200. COL1 fluorescence
525 quantification. Significance vs Basal: ***, $p<0.001$. Significance TENO ESW vs TENO: °, $p<0.05$.
526 Immunoblotting for COL1 (panel B) in cultured media from Basal, ESW, TENO and TENO ESW-
527 treated hASC cells. Red Ponceau was used to confirm equal loading. Blot is representative of five
528 independent experiments. Semiquantitative analysis of immunoblotting results (panel C).
529 Significance vs Basal: ***, $p<0.001$. Significance TENO ESW vs TENO: °°, $p<0.01$. Tenocytes
530 were used as positive controls.

Figure 5. Effects on type I collagen after 5 weeks. Immunofluorescence for COL1 (panel A) in Basal, ESW, TENO and TENO ESW-treated hASC cells. Magnification x200. COL1 fluorescence quantification (panel B). Significance vs Basal: **, $p<0.01$ ***, $p<0.001$. Significance vs TENO: °°°, $p<0.001$. Masson trichrome staining (panel C) of Basal, ESW, TENO and TENO ESW-treated hASC cells. Collagen fibers are indicated by arrows. Magnification x200. Masson trichrome quantification (panel D). Significance vs Basal: **, $p<0.01$ ***, $p<0.001$. Significance TENO ESW vs TENO: °°°, $p<0.001$.

Figure 6. Effects on integrin gene expression. mRNA expression of ITGα2 (panel A), ITGα6 (panel B), ITGβ1 (panel C) was evaluated by RT-PCR. Results are normalized for three different housekeeping genes (β-actin, RPLPO and L13A) and expressed as relative expression fold *vs* Basal. Significance *vs* Basal: *, $p<0.05$; **, $p<0.01$; ***, $p<0.001$. Significance *vs* ESW: $^{\#}$, $p<0.05$; $^{\#\#}$, $p<0.01$; $^{\#\#\#}$, $p<0.001$. Significance TENO ESW vs TENO: °°, $p<0.01$; °°°, $p<0.001$.

Figure 7. Effects on BMP-2 (panel A), Runx2 (panel B) and ALP (panel C) gene expression. mRNA expression was evaluated by RT-PCR. Results are normalized for three different housekeeping genes (β-actin, RPLPO and L13A) and expressed as relative expression fold *vs* Basal. Significance vs Basal: **, $p<0.01$; ***, $p<0.001$. Significance TENO ESW vs TENO: °, $p<0.05$. **Effect on calcium deposition (panel D):** Calcium deposits at 4 weeks (arrows) as revealed by Alizarin Red Staining. Magnification x400. Staining is representative of five independent experiments.

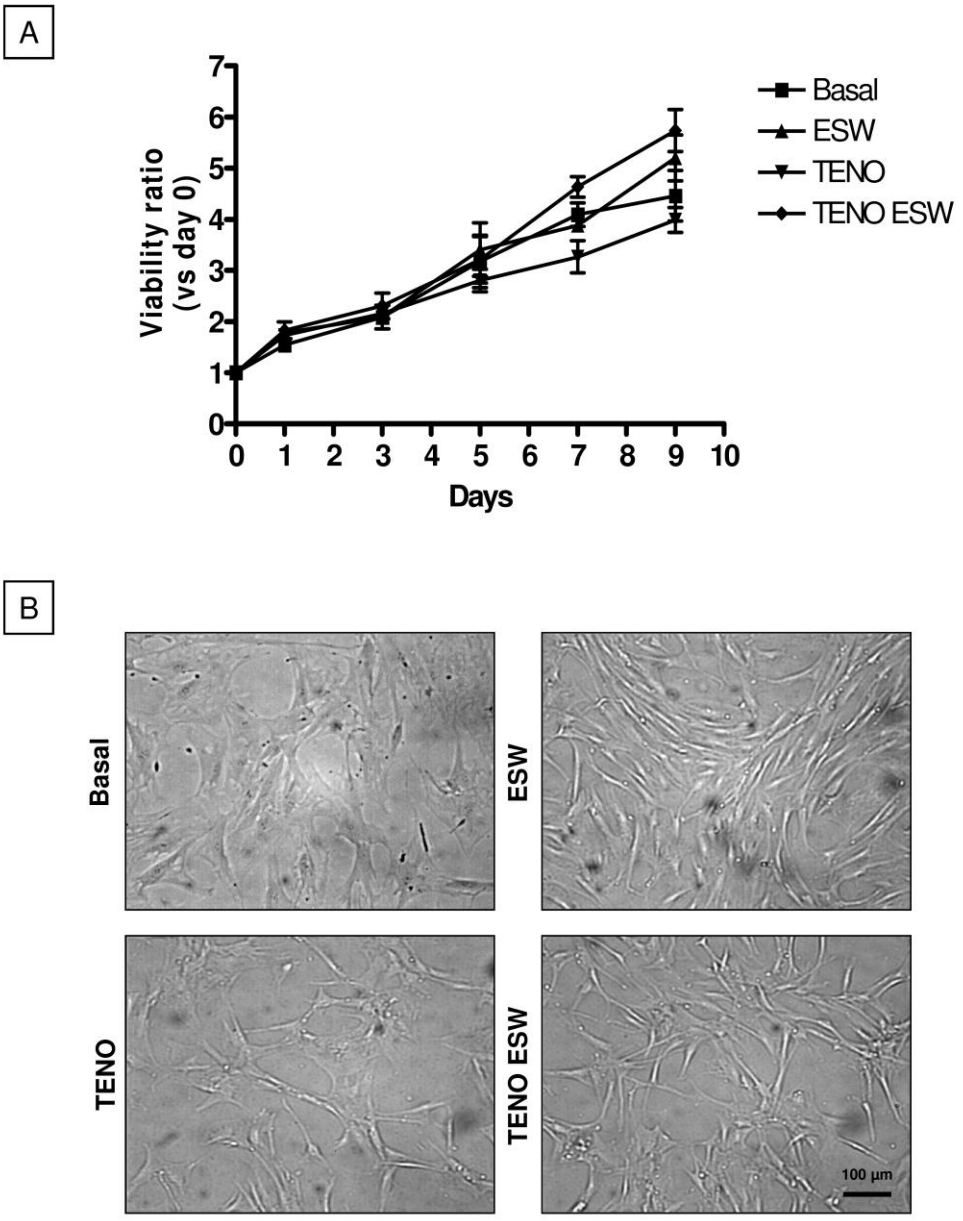
A
Viability ratio
(vs day 0)
Days
Basal
ESW
TENO
TENO ESW
B
Basal
ESW
TENO
TENO ESW
100 µm

Figure 1

551

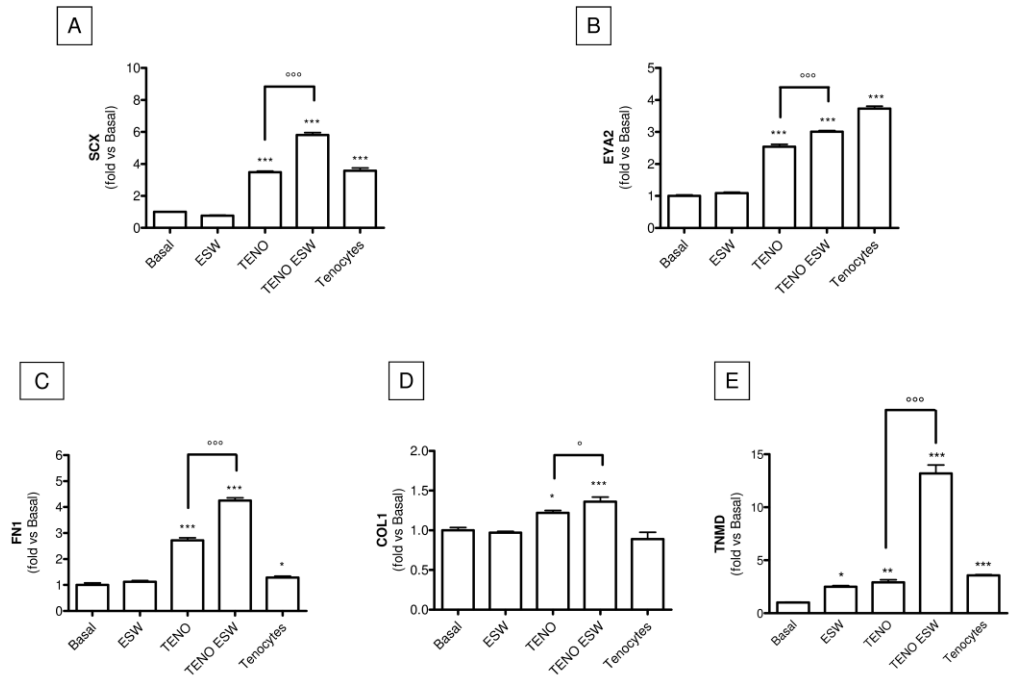

Figure 2

552

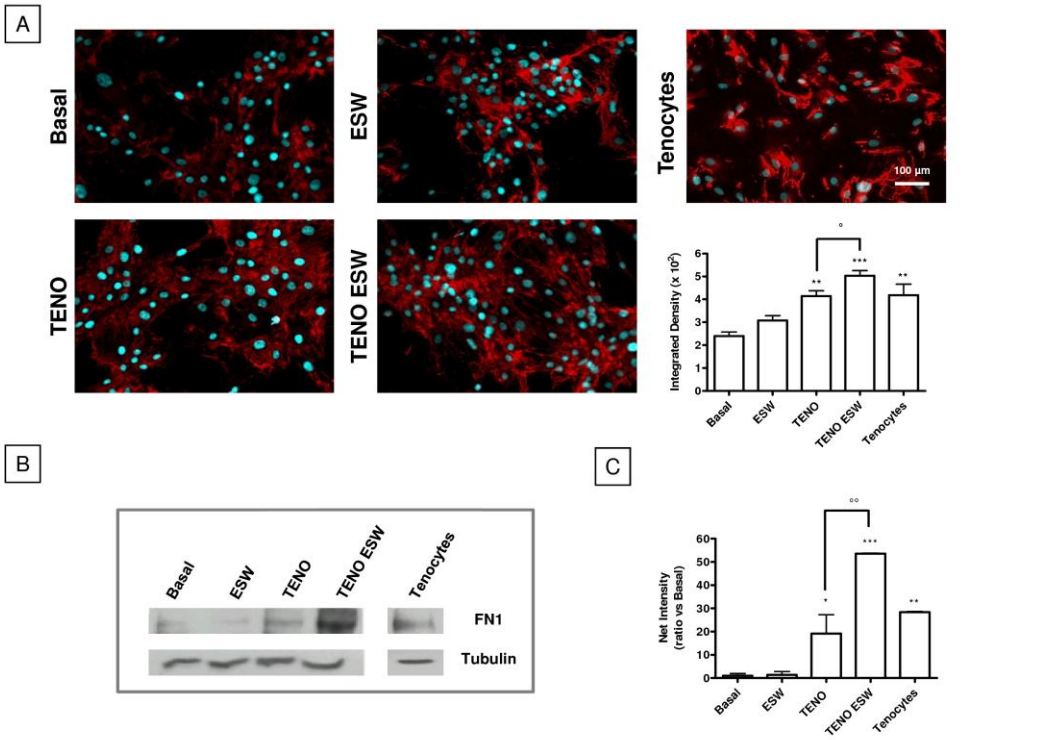

Figure 3

553

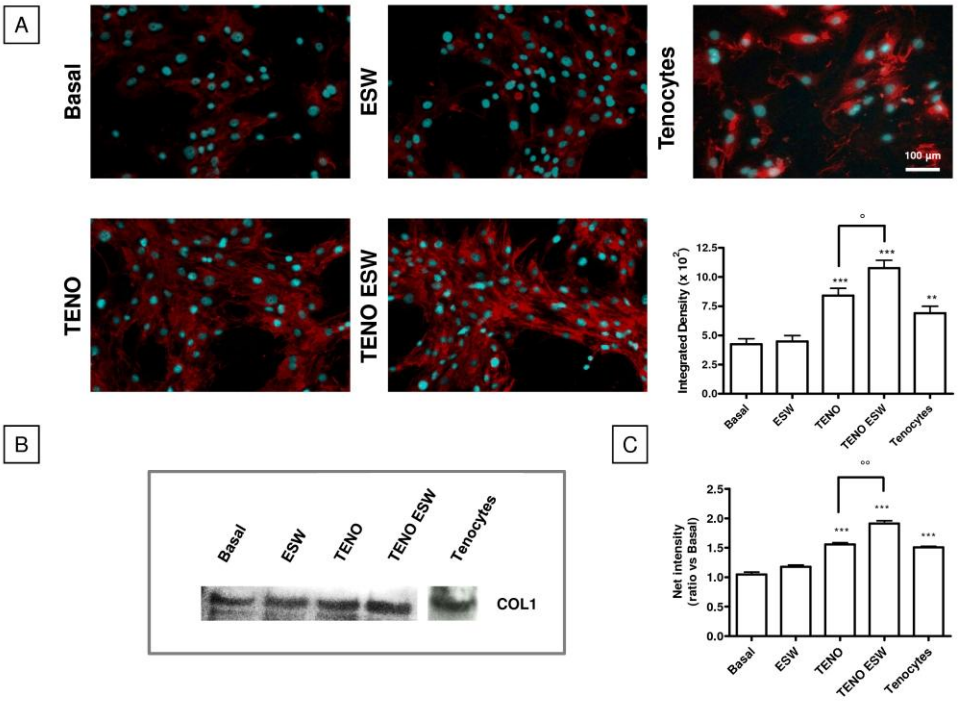

Figure 4

554

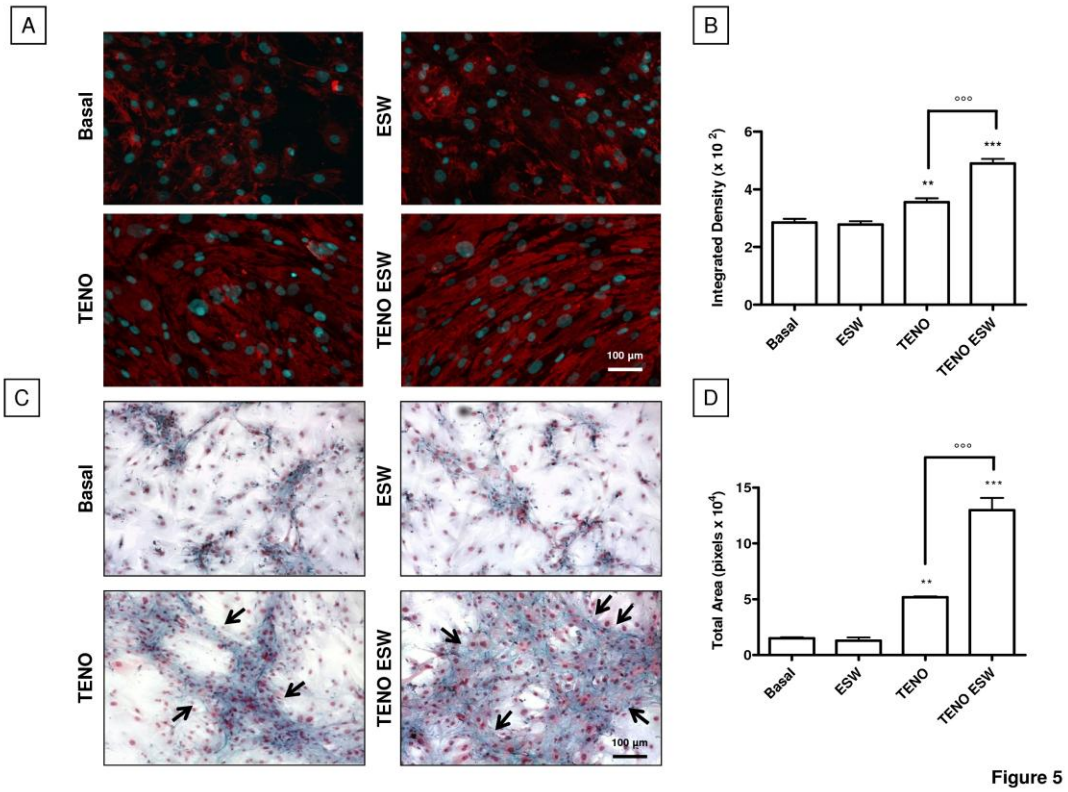

Figure 5

555

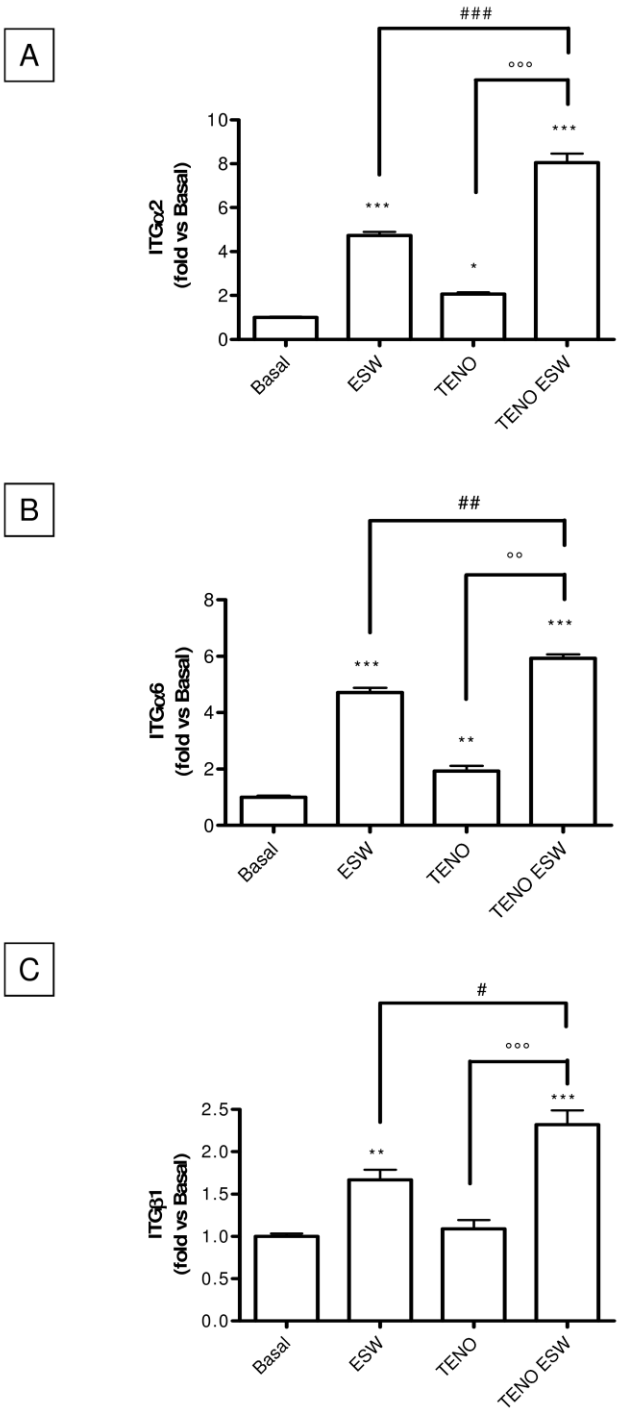
A
###
°°°
***
***
*
ITGα2
(fold vs Basal)
10
8
6
4
2
0
Basal
ESW
TENO
TENO ESW
B
##
°°
***
***
**
ITGα6
(fold vs Basal)
8
6
4
2
0
Basal
ESW
TENO
TENO ESW
C
#
°°°
***
**
ITGβ1
(fold vs Basal)
2.5
2.0
1.5
1.0
0.5
0.0
Basal
ESW
TENO
TENO ESW

Figure 6

556

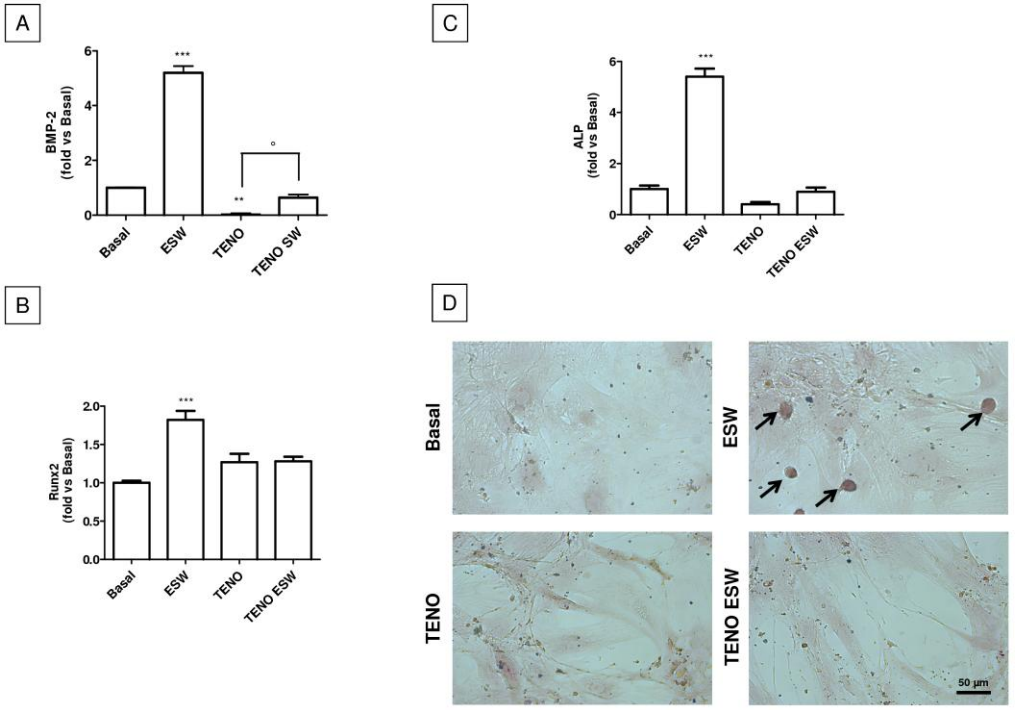

Figure 7

Table S1 Primers for real-time PCR

Gene	Primer sequence	NCBI Reference
SCX	Sense: 5'-GAA CAC CCA GCC CAA ACA GATC-3' Antisense: 5'-GCG GTC CTT GCT CAA CTT TCT C-3'	NM_001080514.2
EYA2	Sense: 5'-GAT TGA GCG TGT GTT CGT GTG G-3' Antisense: 5'-GTG GTG TCC TTC CCG TAT CTG G-3'	NM_005244.4
FN1	Sense: 5'-CCG TGG CAT TGG GGA GTG G-3' Antisense: 5'-GGG TGG GAG TTG GGC TGA C-3'	NM_212482.2
COL1	Sense: 5'-ATG GAT GAG GAG ACT GGC AAC C-3' Antisense: 5'-GGA AGG GCA GGC GTG ATG G-3'	NM_000089.3
TNMD	Sense: 5'-ACGGATACACTGGCATCTACTTCG-3' Antisense: 5'-GGGACCCAAATCACTGACTGTTC-3'	NM_022144

ITGα1	Sense: 5’-ACA TGG GAA CAG AGA AGG AGG AG-3’ Antisense: 5’-TGA ATT GTG CTG CCG AGA TGA AC-3’	NM_181501.1
ITGα2	Sense: 5’-TGT AGC AAC ATC CCA GAC ATC CC-3’ Antisense: 5’-GCA CTT CGT CGC CCA CCA G-3’	NM_002203.3
ITGα5	Sense: 5’-CGG GCT CCT TCT TCG GAT TCT C -3’ Antisense: 5’-CAC TCC TGG CTG GCT GGT ATT AG -3’	NM_002205.4
ITGα6	Sense: 5’-TCC TAC CCT GAT GTT GCT GTT GG-3’ Antisense: 5’-TCT GGC GGA GGT CAA TTC TGT TAG-3’	NM_001079818.2
ITGα10	Sense: 5’-GGG AAC CGA AGA GGG CAG TG -3’ Antisense: 5’-ACA GGC AGA AGA CAA GGA GAG C -3’	NM_003637.4
ITGα11	Sense: 5’-GCA GGC AGT GAC AGT AAT GAG C -3’ Antisense: 5’-CGT ATT TGA GGT GGA AGC GTA AGG -3’	NM_001004439.1
ITGαV	Sense: 5’-TAG CGT ATC TGC GGG ATG AAT CTG -3’ Antisense: 5’-GGC GTG AAC TGG TTA AGA ATG GG -3’	NM_002210.4
ITGβ1	Sense: 5’-TGC CTT GGT GTC TGT GCT GAG-3’ Antisense: 5’-CAA CAG TCG TCA ACA TCC TTC TCC-3’	NM_002211.3
ITGβ3	Sense: 5’-CTT CAA TGC CAC CTG CCT CAA C -3’ Antisense: 5’-GGA CAG CCT CGC ACC TTG G -3’	NM_000212.2
ITGβ5	Sense: 5’-TGC CTG CTG CTC CAC TCT G -3’ Antisense: 5’-AGC CTC CTG GTC ATC TTT CAC G -3’	NM_002213.4
ITGβ8	Sense: 5’-GTG TGT GGA AGG TGT GAG TGC -3’ Antisense: 5’-TGA GAC AAA TTG TGA GGG TGA AGG -3’	NM_002214.2
BMP-2	Sense: 5’-CGG GAG AAG GAG GAG GCA AAG -3’ Antisense: 5’-GAA GCA GCA ACG CTA GAA GAC AG -3’	NM_001200.3
Runx2	Sense: 5’-CGG AGT GGA CGA GGC AAG AG-3’ Antisense: 5’-AGG CGG TCA GAG AAC AAA CTA GG -3’	NM_001024630.3

ALP	Sense: 5'-ATG AGG CGG TGG AGA TGG AC -3' Antisense: 5'-CAT ACA GGA TGG CAG TGA AGG G -3'	NM_000478.5
β-ACT	Sense: 5'-GCG AGA AGA TGA CCC AGA TC- 3' Antisense: 5'- GGA TAG CAC AGC CTG GAT AG-3'	NM_001101.3
L13A	Sense: 5'-GCA AGC GGA TGA ACA CCA ACC-3' Antisense: 5'-TTG AGG GCA GCA GGA ACC AC-3'	NM_012423.3
RPLPO	Sense: 5'-CGA CAA TGG CAG CAT CTA CAA CC-3' Antisense: 5'-CAC CCT CCA GGA AGC GAG AAT G-3'	NM_001002.3

562
563
564
565
566
567 **Table S2.** Mesenchymal stem cell marker expression
568
569

CD 13	98.2 % ± 3.5
CD 14	1.3% ± 0.4
CD 34	NEG
CD 44	99.3 % ± 0.6
CD 45	NEG
CD 90	96.9 % ± 0.1
CD 105	96.8 % ± 2.6

570
571 **Table S3** Cell viability
572
573
574
575
576

Treatment	**Viable cells**
Basal	98.3%
ESW	83%
TENO	97.6%
TENO ESW	82.1%